minerals

MDPI

Communication

Desiccator Volume: A Vital Yet Ignored Parameter in $CaCO_3$ Crystallization by the Ammonium Carbonate Diffusion Method

Joe Harris [1] and Stephan E. Wolf [1,2,*]

[1] Department of Materials Science and Engineering, Institute of Glass and Ceramics (WW3), Friedrich-Alexander University Erlangen-Nürnberg (FAU), Martensstrasse 5, Erlangen 91058, Germany; joe.harris@fau.de

[2] Interdisciplinary Center for Functional Particle Systems (FPS), Friedrich-Alexander University Erlangen-Nürnberg (FAU), Haberstrasse 9a, Erlangen 91058, Germany

* Correspondence: stephan.e.wolf@fau.de; Tel.: +49-9131-85-27565

Received: 30 May 2017; Accepted: 14 July 2017; Published: 19 July 2017

Abstract: Employing the widely used ammonium carbonate diffusion method, we demonstrate that altering an extrinsic parameter—desiccator size—which is rarely detailed in publications, can alter the route of crystallization. Hexagonally packed assemblies of spherical magnesium-calcium carbonate particles or spherulitic aragonitic particles can be selectively prepared from the same initial reaction solution by simply changing the internal volume of the desiccator, thereby changing the rate of carbonate addition and consequently precursor formation. This demonstrates that it is not merely the quantity of an additive which can control particle morphogenesis and phase selectivity, but control of other often ignored parameters are vital to ensure adequate reproducibility.

Keywords: crystal growth; amorphous calcium carbonate; colloidal crystals

1. Introduction

Nature precisely controls crystallization pathways to form functional crystalline materials with non-equilibrium morphologies that feature properties which often exceed those of their artificial counterparts [1–3]. As a consequence, significant research efforts have focused upon the synthesis and characterization of ordered structures of assembled crystallites which mimic the architectures found in nature [4,5]. Typically, organic and inorganic additives are employed to guide polymorph selection and crystallite assembly. These additives are selected based on their ability to favor formation of amorphous phases, interact with growing crystal faces, or assemble into architectures which guide crystal formation. In nature, numerous organic molecules are found in the crystallization milieu, a quantity which reflects the complexity of the mineralization processes performed by the biomineralizing organism [6]. Extraction, isolation, and identification of these molecules is a complex and time intensive process and quite often insufficient material can be extracted to assess the role the molecule takes during crystallization. Nevertheless, crystallization in the presence of such additives is an intensively studied topic, particularly in the case of the most prevalent biomineral calcium carbonate. Work often focuses on how relative quantities of such additives affect crystallization pathways and promote the formation of amorphous phases. Biomineralizing organisms however, do not merely regulate the quantities of additives within the crystallization milieu; they also control the kinetics of the process by mediating the rate at which ions are added. The effect of reaction kinetics on formation and morphogenesis of crystals in the presence of such additives is a much less discussed and well understood process than additive quantity, and is a parameter that is often omitted from studies.

Herein, we demonstrate that alteration of the rate at which carbonate concentration in the reaction solution is increased changes the polymorph selectivity and morphogenesis of calcium carbonates.

To do so, we employed the well-known ammonium carbonate diffusion method in which vessels containing calcium ion containing solutions are sealed in desiccator with vials of ammonium carbonate powder. Decomposition of the powder into carbon dioxide and ammonia, and subsequent absorption of these gaseous molecules into the solution increases carbonate ion concentration and maintains an alkaline pH of the solution. In this study, to vary the reaction kinetics, the size of the desiccator was simply altered. By decreasing the volume of the desiccator, the rates at which both the atmosphere in the desiccator becomes saturated with gas and the carbonate concentration in the solution increases are both increased and the kinetics of carbonate precipitation are influenced. To demonstrate how reaction kinetics can easily influence the effect of an additive on the crystallization system, we selected the magnesium ion as a simple additive. Previous work has shown that magnesium ions interacts with calcium carbonate during formation and stabilizes amorphous phases [7].

2. Materials and Methods

2.1. Materials

Double deionized water (Milli-Q) was used throughout all experiments. Ammonium carbonate (Carl Roth, Karlsruhe, Germany), calcium chloride dihydrate (Merck, Darmstadt, Germany), magnesium chloride hexahydrate (Sigma Aldrich, St. Louis, MO, USA), and hydrochloric acid (Carl Roth) were used without further purification. Glassware was first cleansed with deionized water, immersed in 1 M HCl for 5 min and then rinsed with deionized water before air drying.

2.2. Carbonate Precipitation

In a typical experiment, calcium carbonate precipitation was performed in a desiccator of 21, 11.5 or 3 dm^3 internal volume at 25 °C, for 24 to 72 h. A 9 cm diameter petri dish with a height of 1.2 cm was used as a crystallization vessel. An aqueous 25 mL reaction solution of composition 10 mM $CaCl_2 \cdot 2H_2O$ and 100 mM $MgCl_2 \cdot 6H_2O$ was poured into the petri dish which was then covered with cling film that was punctured with one needle hole 0.9 mm in diameter in the center. One glass vial (10 mL) containing 3 g of freshly crushed ammonium carbonate powder was covered with parafilm punctured with a single hole and placed at the bottom of the desiccator. The petri dish was then placed onto a plate above the glass vial and the desiccator was sealed, effectively starting the reaction. After the desired time, the precipitates were recovered from the air–water interface by use of a glass slide with careful attention paid to prevent aggregation of the particles. The particles were then rinsed with ethanol and air dried. In addition, particle assemblies were also examined by light microscopy whilst still at the air–water interface. Control measurements in the absence of magnesium were performed as above but with the omission of magnesium ions from the reaction solution, but with 200 mM NaCl in the solution to maintain the ionic strength.

2.3. Characterization

Optical microscopy was performed on an Olympus BX51 polarized optical microscope equipped with an Olympus XC50 digital camera (Olympus, Tokyo, Japan). Scanning electron microscopy was performed using a Quanta 200 scanning electron microscope (FEI, Brno-Černovice, Czech Republic) equipped with an energy dispersive X-ray analysis detector on gold sputtered samples mounted on SEM stubs using carbon pads. Powder X-ray diffraction patterns were recorded on a Kristalloflex D500 diffractometer (Siemens, Mannheim, Germany) using monochromatic Cu Kα radiation, (λ = 1.54184 Å) at a scan rate of 1 min^{-1} between 10° and 70°. Infrared spectra were obtained between 600 and 4000 cm^{-1} on a Nicolet iS10 infrared spectrometer equipped with an attenuated total reflection (ATR) accessory (Thermofisher Scientific, Waltham, MA, USA).

2.4. Carbonate Dissolution Quantification

The temporal evolution of the reaction solution pH as a result of ammonium carbonate dissolution was measured using a 905 Titrando titration device equipped with a micro pH probe (Metrohm, Herisau, Switzerland) and recorded on tiamo 2.4 software. Prior to each assay, the probe was calibrated against three standardized buffers of pH 7, 9, and 10. For each desiccator system, a 9 cm diameter petri dish with a height of 1.2 cm was used as a crystallization vessel. An aqueous 25 mL reaction solution of composition 10 mM $CaCl_2{\cdot}2H_2O$ and 100 mM $MgCl_2{\cdot}6H_2O$ was poured into the petri dish which was then covered with cling film that was punctured with two needle holes in the centre, one to allow ammonium carbonate influx and the second to allow the pH probe to be placed in solution. One glass vial (10 mL) containing 3 g of freshly crushed ammonium carbonate powder was covered with parafilm punctured with a single hole and placed at the bottom of the desiccator. The petri dish was then placed onto a plate above the glass vial and the desiccator was sealed, effectively starting the reaction. The solution pH was monitored for 3 h with pH measurements recorded every 5 s. Carbonate content was then calculated from a calibration curve constructed from pH measurements of 10 mL solutions of composition 10 mM $CaCl_2{\cdot}2H_2O$ and 100 mM $MgCl_2{\cdot}6H_2O$ with known quantities of ammonium carbonate.

3. Results

The temporal dissolution of ammonium carbonate into the reaction solution for each of the three desiccator volumes was studied by monitoring the evolution of solution pH against time (Figure S1). Dissolution of ammonia gas into water results in an increase in solution pH. By monitoring the change in solution pH the rate of ammonium carbonate dissolution (Figure 1) could be calculated by use of a calibration curve constructed from pH measurements of solutions of composition 10 mM $CaCl_2{\cdot}2H_2O$ and 100 mM $MgCl_2{\cdot}6H_2O$ and known quantities of ammonium carbonate. The rates of ammonium carbonate dissolution were 0.045, 0.080, and 0.115 mM·min^{-1} for the large, medium, and small desiccators respectively. An increase in internal volume of the desiccator decreased the rate at which ammonium carbonate dissolution into the solution occurred. The ammonium carbonate dissolution rates are lower than the 0.6 mmol·min^{-1} reported previously [8], in which a chamber of lower internal volume was used and the reaction solution and ammonium carbonate were uncovered. These observed differences in dissolution rates highlight the role of desiccator size on determining the rate of carbonate addition into solution.

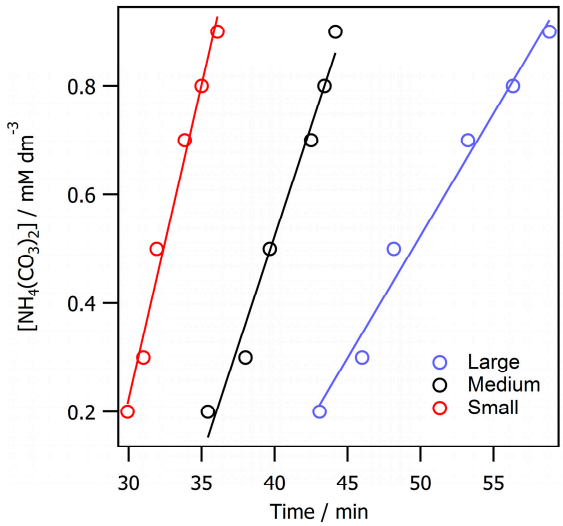

Figure 1. Ammonium carbonate dissolution rates. Temporal evolution of ammonium carbonate concentration for each of the three desiccators; rates of dissolution are 0.045, 0.080, and 0.115 mM·min^{-1} for the large, medium, and small desiccators respectively.

To demonstrate how desiccator size can highly impact $CaCO_3$ saturation levels in the reaction solution, and potentially $CaCO_3$ crystallization pathways, the formation and morphogenesis of calcium carbonate particles precipitated at the air-water interface were investigated. Scanning electron microscopy (SEM) studies of the precipitates removed from solution after 72 h revealed that alteration of the size of the desiccator resulted in the formation of precipitates with differing morphologies and states of crystallinity. In the largest desiccator (21 dm^3 internal volume), roughly spherical polycrystalline grains composed of radially arranged fibres typical of spherulitic growth were observed (Figure 2a). The powder X-ray diffraction (PXRD) pattern of the dried precipitate showed reflections at 2θ = 26.3°, 27.3°, 31.2°, 33.3°, 36.2°, 37.5°, 38.0°, 38.6°, 41.4°, 43.0°, 44.0°, 48.5°, 50.4°, 52.6°, and 53.0° corresponding to the miller indices {111}, {021}, {002}, {012}, {200}, {031}, {112}, {130}, {211}, {132}, {113}, and {231} of aragonite respectively (Figure 3a). The high concentration of magnesium ions in the crystallization solution is known to favour the formation of aragonite instead of the more thermodynamically stable polymorph calcite. This is because Mg^{2+} is incorporated into the calcite lattice but not into the lattice of aragonite, this therefore increases the solubility of calcite and decreases its growth rate at the expense of aragonite [9]. When the volume of the desiccator was reduced to 11.5 dm^3 (herein referred to as medium desiccator), SEM studies on particles extracted from the air-water interface after 72 h revealed that aggregates of particles of no defined shape were formed, and that these aggregates were several hundred micrometers in diameter (Figure 2b). The PXRD pattern (Figure 3a) of these precipitates was devoid of any peaks, and the infrared (IR) spectra (Figure 3b) showed bands at 859 (v_2), 1082 (v_1), 1394 (v_3), and 1633 cm^{-1} (water) and a broad absorbance centered at 3300 cm^{-1} (OH stretch) indicating that particles are highly-hydrated magnesium–substituted amorphous calcium carbonate. Absorbance at 747 and 714 cm^{-1} characteristic of the v_4 bands of crystalline calcium carbonate polymorphs vaterite and calcite respectively were not observed. Further reduction of the volume of the desiccator to 3 dm^3 (herein referred to as small desiccator), resulted in the formation of hexagonally-packed aggregates of spherical particles at the air–water interface after 72 h (Figure 2c). PXRD patterns (Figure 3a) of the dried aggregates contained no peaks, and IR spectra of the aggregates showed bands at 860 (v_2), 1087 (v_1), 1375 (v_3), 1631 (water), and 3300 cm^{-1} (OH stretch) again indicating that the particles are highly-hydrated magnesium-substituted amorphous calcium carbonate. The presence of magnesium in the particles is confirmed by a magnesium peak in the energy dispersive X-ray analysis spectra recorded from the aggregates (Figure S2). This demonstrates the importance of reaction kinetics for not only polymorph selection, as the large and small desiccators contained different polymorphs, but also in morphogenesis as the small and large desiccators contained particles of the same polymorph, but differing morphologies. The IR bands from the precipitate formed in the medium desiccator are at higher wavenumbers than the corresponding bands of the precipitates formed in the small desiccator. This shift is indicative of a higher magnesium content of the precipitates produced in the small desiccator [7]. SEM studies performed on samples from control experiments where magnesium ions where omitted from the reaction solution resulted in the formation of a mixture of rhombohedral calcite and quasi-spherical polycrystalline vaterite at the air–water interface after 72 h (Figure 2d), regardless of the size of desiccator used. This demonstrates that in the absence of Mg the change in desiccator size, and concomitant change in $CaCO_3$ saturation levels, were not sufficient to promote formation of different $CaCO_3$ polymorphs and morphologies after the 72 h of reaction, and that a strong $CaCO_3$ modulating additive such as Mg is required in addition to drive the formation of different structures.

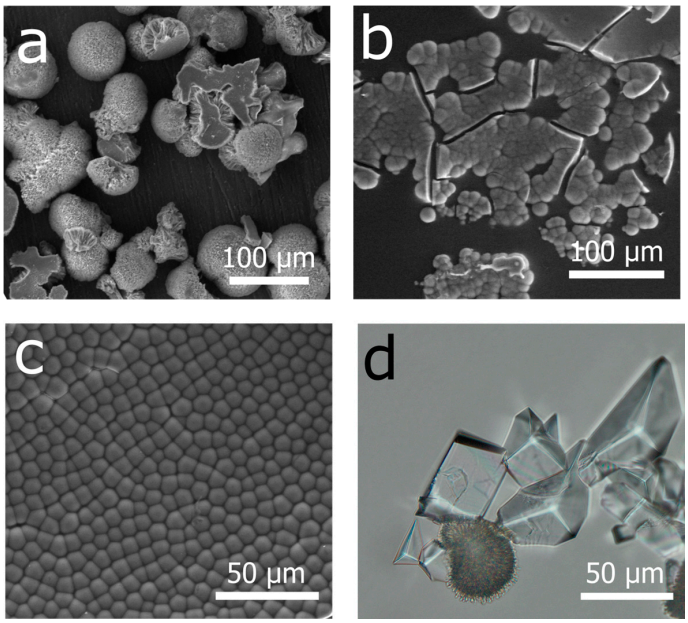

Figure 2. Particles precipitated at the air-water interface after 72 h. (**a**) SEM image of aragonite particles precipitated in the large desiccator; (**b**) SEM image of highly hydrated magnesium-substituted amorphous calcium carbonate precipitated in the medium desiccator; (**c**) SEM image of hexagonally-packed spherical highly hydrated magnesium-substituted amorphous calcium carbonate particles precipitated in the small desiccator; (**d**) Optical microscopy image of representative calcite and vaterite particles precipitated in the large desiccator after 72 h.

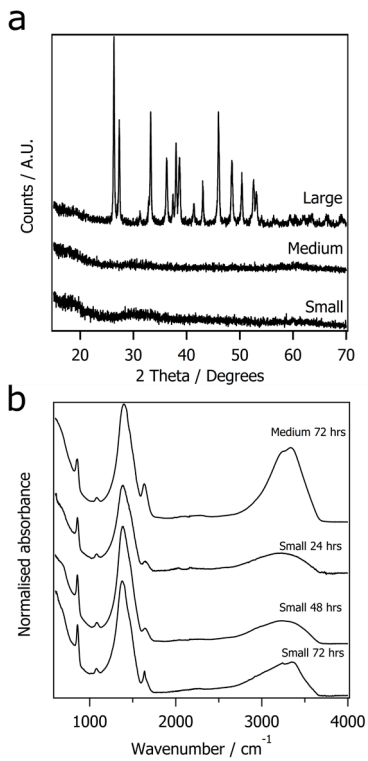

Figure 3. PXRD patterns and IR spectra of particles formed at air-water interface. (**a**) PXRD patterns of precipitates removed from the air-water interface after 72 h from reaction vessels in the small, medium, and large desiccators; (**b**) IR spectra of precipitates removed from the small and medium desiccator at varying time points.

Further studies were undertaken to probe the temporal evolution of structures in the small desiccator system. After 24 h a mixture of micrometre scale spherical particles (1.01 ± 0.24 µm diameter) and aggregates of no defined morphology were present at the air water interface (Figure 4a,d). IR spectra exhibited bands at 852 (v_2), 1098 (v_1), 1398 (v_3), and 1665 cm^{-1} and a broad absorbance centred at 3300 cm^{-1} (Figure 3b) concomitant with hydrated and magnesium-substituted amorphous calcium carbonate. Extension of the reaction time to 48 h resulted in the growth of the spherical particles to an average diameter of 5.78 ± 1.06 µm diameter (Figure 4b,d), and dissolution of the misshapen aggregates so that the most prevalent structure at the air–water interface were the spherical particles. The IR spectra featured bands at 852 (v_2), 1100 (v_1), 1397 (v_3), and 1659 cm^{-1} and a broad absorbance centered at 3300 cm^{-1} (Figure 3b). Further extension of the reaction time to 72 h resulted in increased growth of the spherical particles to 9.45 ± 1.07 µm (Figure 4c,d). The increase in mean particle size resulted in aggregation of the particles at the air-water interface due to the increased surface area occupied by the colloids. Packing of the particles was observed to be largely hexagonal, however, some defects in the colloidal crystal could be observed due to particle movement resulting from incomplete coverage of the air-water interface by the particles. Nevertheless, this demonstrates that colloidal crystals of calcium carbonate can be generated in the absence of an organic additive by control over precipitation rates.

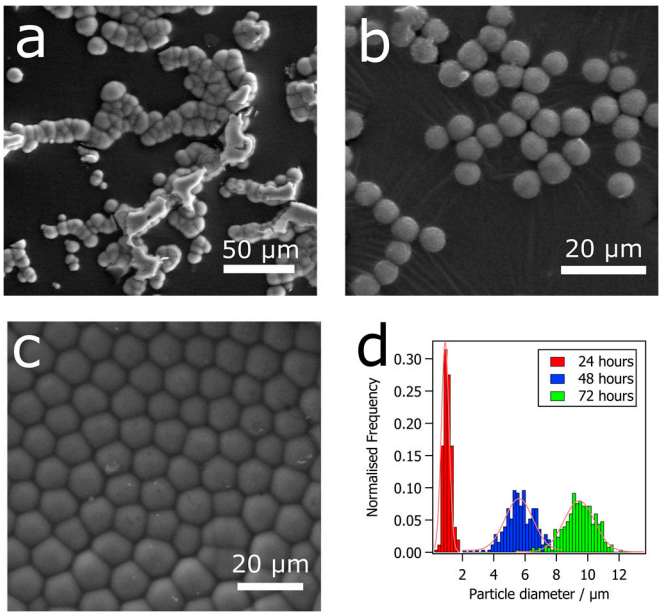

Figure 4. Growth and aggregation of spherical magnesium-calcium carbonate in the small desiccator. (**a**,**b**) SEM images of particles formed at the air-water interface in the small desiccator after 24 and 48 h, respectively; (**c**) Optical microscopy image of spherical particles at the air water interface after 72 h; (**d**) A histogram of particle sizes measured from optical microscopy images after 24, 48, and 72 h.

In conclusion, this report demonstrates that hexagonally packed arrays of spherical magnesium-doped amorphous calcium carbonate particles or spherulitic aragonite particles can be selectively synthesized from the same magnesium and calcium bearing solution by altering the size of the desiccator used. This shows that use of a simple additive (Mg ions) in combination with precise reaction kinetics is sufficient to generate higher-order structures and indicates even more elaborate structures can be generated by the combination of more complex additives and control over reaction kinetics. Moreover, this report highlights how the endemic problem of reproducibility can develop between laboratories, even for simple crystallization procedures. Often, vital experimental parameters are simply omitted from reports either through complacency or due to a lack of perception of their importance. Here, we have altered the size of the desiccator used, an extrinsic experimental

parameter which is rarely disclosed in reports, yet one that is shown to be an essential variable which can drastically change crystallization by altering the reaction kinetics. Other variables associated with the ammonium carbonate diffusion method have been identified and characterized [9], however, the free volume of the reaction chamber remains a parameter which is still neglected. This report therefore demonstrates that an established protocol is required that can be used as an assay to compare crystallization experiments between laboratories. This is essential for systems in which difficult to acquire or expensive additives are used as it will increase reproducibility, thereby increasing research output.

Supplementary Materials: The following are available online at www.mdpi.com/2075-163X/7/7/122/s1, Figure S1: Temporal evolution of solution pH in the large, medium, and small desiccators; Figure S2: Energy dispersive X-ray analysis of magnesium doped amorphous calcium carbonate particles formed at the air-water interface in the small desiccator after 72 h.

Acknowledgments: Stephan E. Wolf acknowledges financial support by an Emmy Noether starting grant issued by the German Research Foundation (DFG, No. WO1712/3-1). Joe Harris and Stephan E. Wolf acknowledge financial support from the Cluster of Excellence 315 "Engineering of Advanced Materials—Hierarchical Structure Formation for Functional Devices" funded by the German Research Foundation. Eva Springer is thanked for assistance with scanning electron microscopy imaging.

Author Contributions: Joe Harris and Stephan E. Wolf conceived and designed the experiments; Joe Harris performed the experiments and analysed the data; Joe Harris and Stephan E. Wolf wrote the paper.

Conflicts of Interest: The authors declare no conflict of interest.

References

1. Ma, Y.; Aichmayer, B.; Paris, O.; Fratzl, P.; Meibom, A.; Metzler, R.A.; Politi, Y.; Addadi, L.; Gilbert, P.U.P.A.; Weiner, S. The grinding tip of the sea urchin tooth exhibits exquisite control over calcite crystal orientation and Mg distribution. *Proc. Natl. Acad. Sci. USA* **2009**, *106*, 6048–6053. [CrossRef] [PubMed]
2. Hovden, R.; Wolf, S.E.; Holtz, M.E.; Marin, F.; Muller, D.A.; Estroff, L.A. Nanoscale assembly processes revealed in the nacroprismatic transition zone of Pinna nobilis mollusc shells. *Nat. Commun.* **2015**, *6*, 10097. [CrossRef] [PubMed]
3. Weaver, J.C.; Milliron, G.W.; Miserez, A.; Evans-Lutterodt, K.; Herrera, S.; Gallana, I.; Mershon, W.J.; Swanson, B.; Zavattieri, P.; DiMasi, E.; et al. The stomatopod dactyl club: A formidable damage-tolerant biological hammer. *Science* **2012**, *336*, 1275–1280. [CrossRef] [PubMed]
4. Lee, K.; Wagermaier, W.; Masic, A.; Kommareddy, K.P.; Bennet, M.; Manjubala, I.; Lee, S.-W.; Park, S.B.; Cölfen, H.; Fratzl, P. Self-assembly of amorphous calcium carbonate microlens arrays. *Nat. Commun.* **2012**, *3*, 725. [CrossRef] [PubMed]
5. Harris, J.; Mey, I.; Hajir, M.; Mondeshki, M.; Wolf, S.E. Pseudomorphic transformation of amorphous calcium carbonate films follows spherulitic growth mechanisms and can give rise to crystal lattice tilting. *CrystEngComm* **2015**, *17*, 6831–6837. [CrossRef]
6. Marie, B.; Joubert, C.; Tayalé, A.; Zanella-Cléon, I.; Belliard, C.; Piquemal, D.; Cochennec-Laureau, N.; Marin, F.; Gueguen, Y.; Montagnani, C. Different secretory repertoires control the biomineralization processes of prism and nacre deposition of the pearl oyster shell. *Proc. Natl. Acad. Sci. USA* **2012**, *109*, 20986–20991. [CrossRef] [PubMed]
7. Loste, E.; Wilson, R.M.; Seshadri, R.; Meldrum, F.C. The role of magnesium in stabilising amorphous calcium carbonate and controlling calcite morphologies. *J. Cryst. Growth* **2003**, *254*, 206–218. [CrossRef]
8. Ihli, J.; Bots, P.; Kulak, A.; Benning, L.G.; Meldrum, F.C. Elucidating mechanisms of diffusion-based calcium carbonate synthesis leads to controlled mesocrystal formation. *Adv. Funct. Mater.* **2013**, *23*, 1965–1973. [CrossRef]
9. Davis, K.J.; Dove, P.M.; De Yoreo, J.J. The role of Mg^{2+} as an impurity in calcite growth. *Science* **2000**, *290*, 1134–1138. [CrossRef] [PubMed]

© 2017 by the authors. Licensee MDPI, Basel, Switzerland. This article is an open access article distributed under the terms and conditions of the Creative Commons Attribution (CC BY) license (http://creativecommons.org/licenses/by/4.0/).